Virology **282,** 102–112 (2001)
doi:10.1006/viro.2000.0809, available online at http://www.idealibrary.com on IDEAL®

Binding Properties, Cell Delivery, and Gene Transfer of Adenoviral Penton Base Displaying Bacteriophage

Monica Di Giovine,*,† Barbara Salone,* Yuri Martina,* Viviana Amati,† Giovanna Zambruno,† Enrico Cundari,‡ Cristina M. Failla,† and Isabella Saggio*,[1]

*University La Sapienza, Department of Genetics and Molecular Biology, Rome, Italy; †Istituto Dermopatico dell' Immacolata, IDI-IRCCS, Laboratory of Molecular and Cell Biology, Rome, Italy; and ‡Centro Genetica Evoluzionistica, CNR, Rome, Italy

Received September 18, 2000; returned to author for revision November 8, 2000; accepted December 19, 2000

The penton base of adenovirus mediates viral attachment to integrin receptors and particle internalisation, properties that can be exploited to reengineer prokariotic viruses for the infection of mammalian cells. We report that filamentous phage displaying either the full-length penton base gene or a central region of 107 amino acids on their surface were able to bind, internalise, and transduce mammalian cells expressing integrin receptors. Both phage bound $\alpha v\beta 3$, $\alpha v\beta 5$, $\alpha 3\beta 1$, and $\alpha 5\beta 1$ integrin subtypes. Cell-binding was shown by electron microscopy; internalisation was investigated by immunofluorescence and confirmed by micropanning. As it has been described for adenovirus, pharmacologic disruption of phosphoinositide-30H kinase, but not of myosin light-chain kinase, inhibited phage internalisation. Recombinant phage encoding an eukaryotic expression cassette was able to mediate gene expression in mammalian cells. Taken together, these data open insights for the exploit of recombinant phage for integrin-targeted gene delivery.

Key Words: integrins; endocytosis; phage-display.

INTRODUCTION

To improve gene therapy efficacy and specificity, substantial effort is currently being addressed to produce modified constructs able to target selected tissues or cell types. To this purpose, viral and nonviral vectors have been engineered, physically or genetically, to display ligand-specific mAbs or receptor-specific peptides (Harari *et al.,* 1999; Hong *et al.,* 1999a; Luo and Saltzman, 2000; Reynolds *et al.,* 1999; Zhang *et al.,* 1998). Crucial information has been derived from these studies. Structural and functional complexity of eukaryotic viruses often hinders the manipulation of capsidic proteins. In the case of retroviral vectors it has been shown that genetic modification of the envelope protein can alter its fusogenic properties, therefore lessening viral infectivity (Russel and Cosset, 1999). The complex structure of the trimeric fibre of adenovirus has allowed only restrained genetic modifications, i.e., small peptides inserted in defined regions of the fibre knob, limiting the available pattern of targeting ligands (Dmitriev *et al.,* 1998, Roelvink *et al.,* 1999). Complete knocking out of vector natural tropism is particularly complex in the case of eukaryotic viruses. The dual adenoviral infectious pathway, for example, sustains residual infectivity of viruses ablated in their primary receptor-binding capacity, through the penton-base integrin interaction (Roelvink *et al.,* 1999).

Filamentous bacteriophage modified to target selected receptors have been recently proposed for gene delivery purposes. In comparison to eukaryotic viral vectors, two major advantages can be anticipated for phage-derived vectors: the easier manipulation of the capsidic proteins and the absence of natural tropism for mammalian cells. Filamentous phage can host exogenous peptides in the capsidic proteins pIII, pVIII, and pVI (Felici *et al.,* 1995; Hufton *et al.,* 1999; Lowman *et al.,* 1991; Lowman and Wells, 1993). We have reported that a neurotrophic factor, hCNTF, can be functionally displayed on phage as a pIII fusion (Saggio *et al.,* 1995b). Recently, it has been demonstrated that phages monovalently displaying fibroblast growth factor-2 (FGF-2) on their coat were able to efficiently deliver a reporter gene into FGF receptor expressing cells (Larocca *et al.,* 1999, 1998). Furthermore, it has been proposed that gene transfer characteristics of recombinant phage can be improved by direct *in vivo* selection of better transducers from library of ligands' variants displayed on phage (Kassner *et al*., 1999).

The adenovirus penton base (Ad-Pb) protein represents an interesting molecule for the production of a highly performant phage-derived mammalian vector. Ad-Pb possesses multiple biological functions: attachment to integrin receptors, internalisation of viral particles, and release of the capsid from endosome (Wickham *et al.,* 1993,

[1] To whom reprint requests should be addressed at Istituto di Genetica, University La Sapienza, Department of Genetics and Molecular Biology, Piazzale Aldo Moro 5, 00185 Rome, Italy. Fax: 0039 06 4456 866. E-mail: saggio@axcasp.caspur.it.

0042-6822/01 $35.00

1994). Two integrin-binding motifs have been identified in Ad-Pb: a central RGD motif and a LDV sequence, positioned between amino acids (aa) 340–342 and 287–289 of Ad serotype 2 pIII, respectively. Adenoviruses are known to exploit the interaction between Pb and the $\alpha v\beta 3$, $\alpha v\beta 5$ integrins for viral entry into cells (Mathias *et al.,* 1998; Wickham *et al.,* 1994). In addition, Ad-binding to hematopoietic cells can be blocked by anti-$\alpha M\beta 2$ antibodies (Huang *et al.,* 1996), while a $\beta 1$-activating antibody rendered melanoma cells more susceptible to adenoviral infection (Davison *et al.,* 1997). Recent data indicate that the integrin $\alpha 6\beta 1$ plays a role in adenoviral infection of the intestinal epithelium (Croyle *et al.,* 1998). The interaction of the virus with integrin receptors plays a key role in infection efficiency, since it mediates viral internalisation. This takes place through the formation of clathrin-coated endocytic vesicles, followed by Ad-mediated vesicle permeabilisation. This process appears to be preferentially mediated by the integrin $\alpha v\beta 5$ (Wickham *et al.,* 1994). Adenovirus internalisation by αv integrins requires activation of phosphoinositide-3-OH kinase (PI3K), a downstream effector of the focal adhesion kinase (FAK), a cell-signalling molecule associated with integrin-mediated cellular processes. On the other hand, adenovirus entry was shown to be independent from the αv integrin-mediated cell motility pathways, i.e., ERK1/ERK2 MAP kinase pathway and myosin light-chain kinase signaling (Li *et al.,* 1998b). Recently, Hong *et al.* have shown that baculovirus-expressed Pb, both as a monomer and as a pentamer, is able to effectuate the entire entry pathway of adenovirion, i.e., enter the cell through the endocytic pathway, promote self-vesicular escape, and target the nucleus crossing the nuclear membrane through the nuclear pores (Hong *et al.,* 1999b). These results have enclosed the possibility of using Pb as a gene delivery molecule, as it has been already proposed for the VP22 of herpesvirus (Elliott and O'Hare, 1997).

We reasoned that, taken together, Pb binding and internalisation properties could confer to bacteriophage vectors' exclusive gene-delivery characteristics for mammalian cells. We therefore constructed recombinant filamentous phages expressing on their surface either the full-length Ad2 Pb (Pb phage) or its central domain (ΔPb phage) and included in the phagemids an eukaryotic expression cassette. The aims of this work were to validate if Pb properties could be exported to a macromolecular assembly different from the adenovirus and to give insight on the potential of Pb-expressing phages as integrin-targeted DNA delivery vectors for mammalian cells.

RESULTS

Phage display of fusion proteins

The full-length Ad2 Pb gene or its central domain (Pb 286–393) were inserted in the phagemid pHenΔ (Hogenboom *et al.,* 1991). Three parameters were considered for the construction of the ΔPb phage: (i) size of the insert, to limit interference with phage functionality; (ii) inclusion of the integrin-binding motif, RGD; and (iii) structural conformation of the insert. To this regard, we took into account literature data on Ad-particles cryo-EM visualisation (Stewart *et al.,* 1997) and performed structure-prediction analysis of the Pb sequence. Taken together, data indicated that the Pb 286–393 stretch would have included the RGD integrin-binding motif surrounded by α-helices, expected to give a structural conformation to the exposed loop. Recombinant phagemids were constructed to present Pb fragments as fusions to the C-terminal coding region of the fd gene *III* (pIII aa 250–406). Bacterial clones transformed with recombinant vectors were infected with a helper phage to produce phage particles monovalently displaying on their surface recombinant Pb–ΔpIII proteins (Lowman *et al.,* 1991). To check the correct expression of recombinant proteins, Western blotting of Pb phage and ΔPb phage was performed using an anti-Pb polyclonal antibody. As shown in Fig. 1, discrete bands could be detected for both Pb and ΔPb phages; band mobility corresponded to the expected molecular weight. Quantification of recombinant pIII/phage preparation was performed, normalizing for protein content on Coomassie blue stained phage pVIII, and, successively comparing Ad-Pb with phage Pb-ΔpIII and ΔPb-ΔpIII blot signals. It could be calculated that

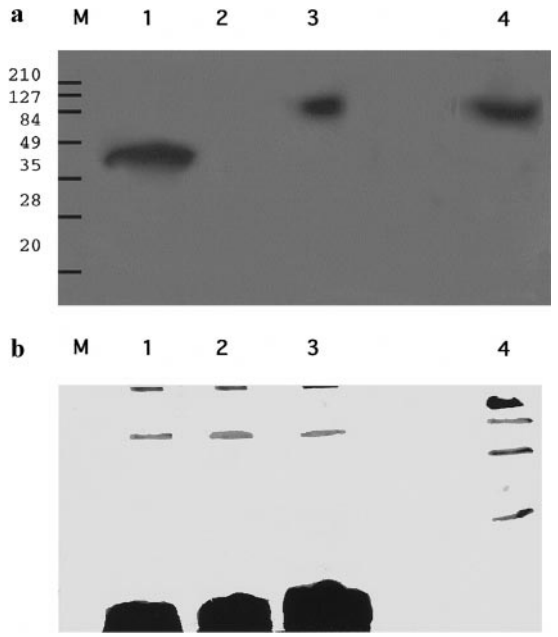

FIG. 1. Recombinant proteins are correctly displayed on phages. (a) 1.2×10^{12} recombinant phage particles were loaded on SDS denaturing gel and immunoblotted; immunodetection was performed with an anti-Pb polyclonal antiserum. (b) 1.2×10^{12} recombinant phage particles were loaded on SDS denaturing gel; proteins were revealed with Coomassie staining. M, molecular weight marker (Kd); lane 1, ΔPb phage; lane 2, control phage; lane 3, Pb phage; lane 4, Adenovirus (1.2×10^9 viral particles).

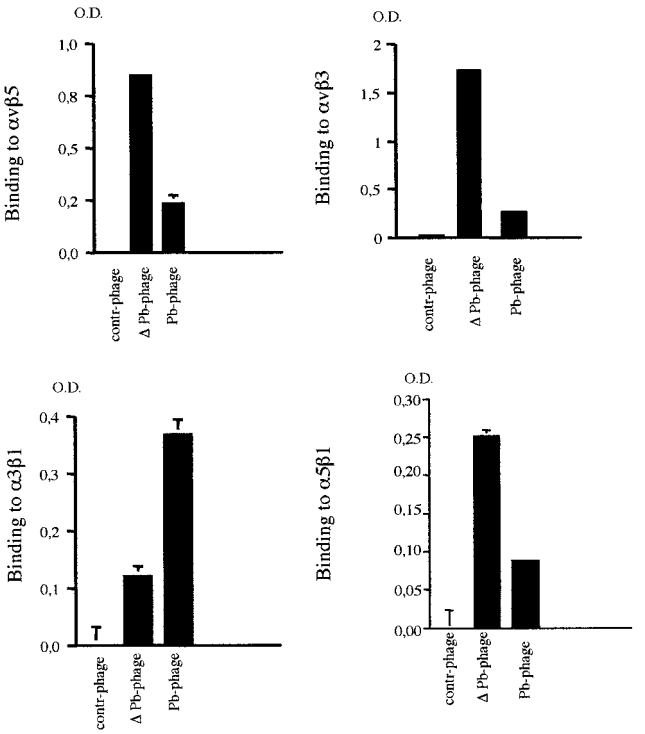

FIG. 2. Recombinant phages bind *in vitro* to integrin receptors. Immobilised integrins were incubated with Pb phage (4×10^{12}), ΔPb phage (1×10^{12} particles/well), or control phage (4×10^{12} particles/well). Bound phages were revealed with an anti-M13 monoclonal antibody. Data are presented as O.D. average values from duplicate measurements; standard deviation is shown.

higher amounts of recombinant pIII were present in ΔPb phage stock as compared to that of Pb phage: 1/23 and 1/118 recombinant pIII/total pIII, respectively. Presumably, the 571 aa insert interferes with viral assembly, and therefore its incorporation into capsids was disadvantaged. Another possibility is that the exogenous Pb moiety impaired phage infectivity. This hypothesis is consistent with the observation that, although titers of both recombinant phages were comparable to those observed for control phages, a time-dependent decrease of infectious titer was noticed for Pb phage (not shown). It could be possible as well that the recombinant Pb-ΔpIII has solubility limitations that decrease the level of incorporation into phage capsids.

Phage binding to integrin receptors *in vitro*

To determine whether the phage represents a compatible scaffold for the functional expression of Pb-derived peptides, and if the Pb (286–393) fragment is sufficient for integrin binding, recombinant phages were tested for their binding activity to integrin receptors *in vitro*.

As shown in Fig. 2, both Pb phage and ΔPb phage were able to bind αvβ3, αvβ5, α3β1, and α5β1 integrins, immobilised on a solid surface. On all integrins tested, no significant binding was observed for control phage. The ratio between Pb-phage and ΔPb-phage signals ranged from 1/4 to 1/5, when binding was performed on αvβ3, αvβ5, and α5β1 integrins. Conversely, a fivefold higher binding for Pb phage, as compared to ΔPb phage, was observed when binding was analysed on the α3β1 integrin. Since direct Ad binding to soluble integrins has been described only for αvβ5 (Mathias *et al.,* 1998), it was particularly relevant to validate the specificity of our data. Competition experiments were performed, using the soluble integrin-binding peptide G*RGD*SP, and a control peptide (G*RGE*SP). As shown in Table 1, significant competition was observed with peptide G*RGD*SP both for Pb phages and for ΔPb phages on each integrin analysed.

Phage binding and internalisation *in vivo*

The ultimate goal of our study was the validation of penton base as an appropriate molecule to reengineer prokaryotic viruses for gene transfer in mammalian cells. We were therefore especially interested in the interaction of Pb phage and ΔPb phage with eukaryotic cells.

HeLa cells were incubated at 4°C with recombinant phage particles and cell sections were analysed by electron microscopy. As shown in Fig. 3, filamentous phage-like structures were visible along cell surface, both when cells were incubated with phages displaying the full penton-base protein (Fig. 3a) and with particles displaying the Pb central loop (Figs. 3b and 3c). At the conditions tested no extracellular filamentous structures were observed on cells incubated with control phages (not shown).

To investigate the ability of phages to be internalised, immunofluorescence studies on cells incubated at 37°C with recombinant phages were performed. Using anti-M13 monoclonal antibodies, a cytoplasmic punctate labeling was observed both in Pb-phage- (Fig. 4a) and in ΔPb-phage- (Fig. 4b) treated cells. In Figs. 4d and 4e are shown the results of the same experiment performed incubating cells with ΔPb phage at 4°C. In these conditions, receptor-mediated endocytosis, an energy depen-

TABLE 1

Specificity of Phage Binding to Integrin Receptors

Competitor peptide	Phage	αvβ3 Binding (% of control)	αvβ5 Binding (% of control)	α3β1 Binding (% of control)
GRGDSP	ΔPb-phage	14	70	37
	Pb-phage	25	58	21
GRGESP	ΔPb-phage	93	94	95
	Pb-phage	62	105	99

Note. 10^{12} phage particles were incubated with purified integrins (0.2 μg/ml) with or without competitors (4.86 μM). Results are expressed as percentages of binding obtained in the absence of competitor.

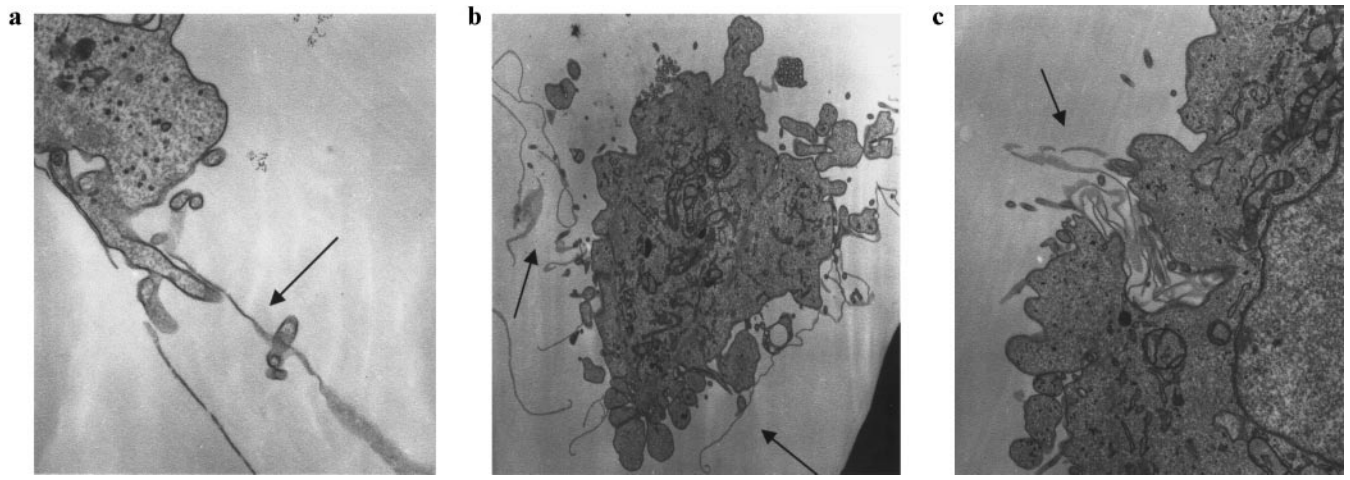

FIG. 3. Electron microscopy detection of phage binding to mammalian cells. 10^5 HeLa cells were incubated at 4°C with 3×10^{12} and 9×10^{12} particles of ΔPb phage (b, c) and Pb phage (a), respectively. After incubation, cells were processed for electron microscopy analysis. Original magnification: a, 15,500×; b, 5200×; c, 11500×.

dent event, is impaired, and labeling was observed all along the cell surface, independently of cell permeabilization prior to antibody addition (Figs. 4d and 4e, respectively). At all temperatures tested, fluorescence intensity in cells incubated with control phages was comparable to background levels.

Quantification of phage binding and internalisation *in vivo*

To further validate phage binding and internalisation properties, micropanning experiments with recombinant and control phages were performed on various cell lines. As a preliminary study, we analysed by FACS integrin display on HeLa, CS-1, CS-1/β3, and Cs-1/β5 cells, using antibodies directed to αvβ3, αvβ5, or β1 integrins. As shown in Fig. 5, CS-1 were found to be negative to all antibodies, while CS-1/β3 and Cs-1/β5 were strongly positive when incubated with an anti-αvβ3 or an anti-αvβ5 antibody, respectively. HeLa cells were found negative for αvβ3 and weakly positive (8.4%) for αvβ5 integrin subtypes, but strongly positive (67.3%) for the β1 subtype.

To quantify binding and internalisation levels on different cell lines, phages were panned on immobilised cells at 4 or 37°C, respectively. When only the internalised fraction had to be analysed, extreme buffer conditions (6 M urea/1 N HCl) were used in washing steps to eliminate phages bound to cell surface. As shown in Table 2, highest Pb-phage binding, and consequent lowest ΔPb-/Pb-phage ratio, was observed in HeLa cells, both in binding and in internalisation. Taking into account the abundant expression of β1 integrins observed in these cells, these results are consistent with *in vitro* data on Pb-phage affinity for the α3β1 integrin (Fig. 2).

Pharmacological analysis of the internalisation pathway

Adenovirus endocytosis *via* the αv integrins requires specific kinase activation. In particular, Ad-integrin binding implies PI3K activation, but not MAP kinase or myosin light-chain signaling (Li *et al.,* 1998a). We performed phage micropanning on HeLa cells treated with kinase inhibitors. As shown in Fig. 6, significant decrease of phage internalisation, as compared to controls, was observed when phage infection was performed in the presence of Wortmannin, an inhibitor of the PI3K kinase (Ui *et al.,* 1995). On the other hand, endocytosis was unaltered when the same experiment was performed in the presence of the myosin light-chain kinase inhibitor, ML7-hydrochloride (ML-7; Saitoh *et al.,* 1987). Taken together, these data suggest that recombinant phages activate the same kinase pathway of adenovirus.

Phage-mediated transduction of mammalian cells

An eukaryotic green fluorescent protein (GFP) expression cassette was inserted in the recombinant phagemids Pb-phenΔ and ΔPb-phenΔ. To analyse transduction efficacy and specificity, Pb-GFP phages or ΔPb-GFP phages were incubated at 37°C with HeLa, Cs-1/β3, or Cs-1 cells. After 72 h, GFP expression was detected by FACS. As shown in Fig. 7a, significant transduction was obtained in HeLa and Cs-1/β3 cells, with a peak of 4% efficiency in HeLa cells transduced with ΔPb-GFP phages. As expected, GFP was not detected in the CS-1 line. To validate receptor specificity of transduction, ΔPb-GFP phage was incubated with HeLa cells in the presence of competing peptides. As shown in Fig. 7b, the G*RGD*SP peptide could inhibit ΔPb-GFP-phage transduction by 90%, while only partial inhibition was obtained with the G*RGE*SP peptide. Taken together these data

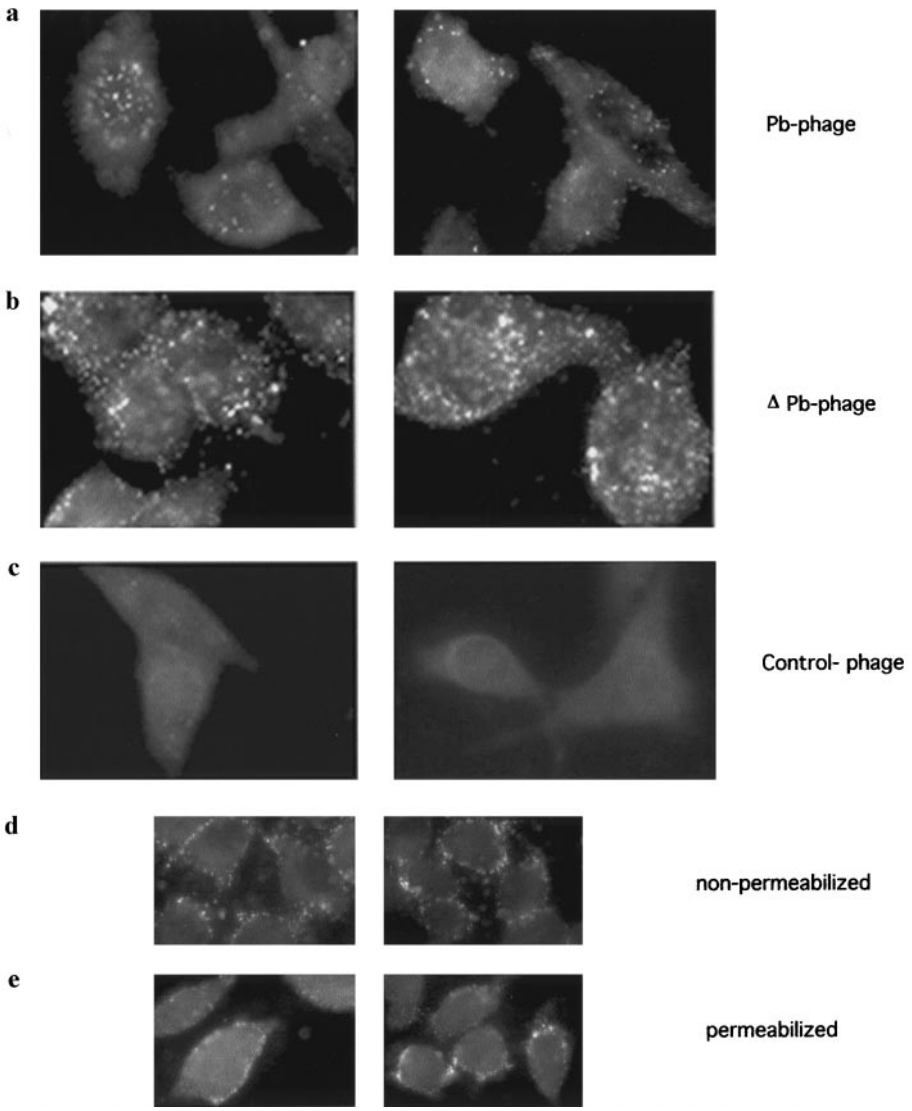

FIG. 4. Immunofluorescence reveals phage internalisation of recombinant phages in mammalian cells. 2.5×10^5 HeLa cells were incubated with phage particles. For control phage (c) and ΔPb phage (b, d, e) 3×10^{12} were used; for Pb phage (a) 9×10^{12}. (a, b, and c) Incubation was performed 1 h at 4°C followed by 1 h at 37°C; antibodies for phage detection were added following cell permeabilization. (d, e) Cells were incubated only 1 h at 4°C to inhibit receptor-dependent phage internalisation. (d) Cells were not permeabilized prior to antibody addition; (e) Cells were permeabilized prior to antibody addition. Cells were examined using a fluorescence microscopy with a 40× objective.

validate recombinant phages as gene transfer vectors for mammalian cells.

DISCUSSION

The penton base protein provides adenovirus the ability to bind and enter the cells and to escape from the endosomes (Wickham *et al.,* 1993). We show in here that filamentous phages can be reengineered to display the penton base protein and that this protein confers to the prokaryotic virus binding and internalisation properties together with gene-delivery capacity for mammalian cells.

The integrin-binding properties of Pb could be transferred to filamentous phages both when the entire molecule was expressed as a monomer on the surface of the virus and when only its central loop was displayed. Direct binding of recombinant phages was shown, both for Pb phage and for ΔPb phage, on adenovirus receptors, $\alpha v\beta 3$ and $\alpha v\beta 5$, and also on $\beta 1$ integrin receptors. Binding specificity was shown by competition ELISA performed in the presence of the G*RGD*SP peptide, which competes the interaction of ligands with the RGD integrin binding motif. Lowest competition was observed when the G*RGD*SP peptide was used to compete phage binding to $\alpha v\beta 5$ integrin. These data are consistent with high binding affinity of the penton base for this integrin subtype (Mathias *et al.,* 1998). As expected, the control peptide G*RGE*SP did not give significant inhibition of

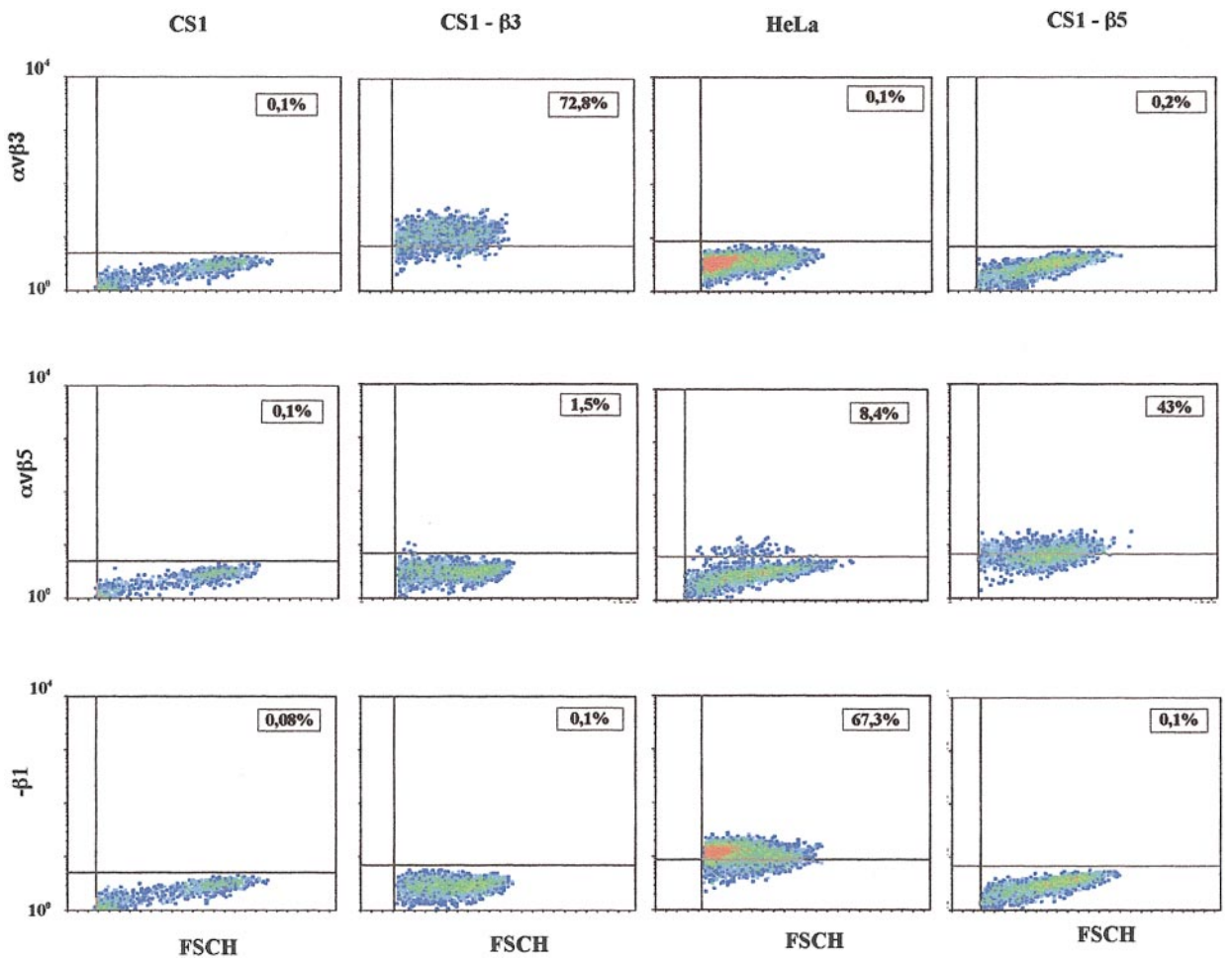

FIG. 5. Differential expression of integrin receptors on Cs-1, Cs-1/β3, HeLa, and Cs-1β5 cells. 1.5 $\times$ 10^5 cells were incubated with one of the following primary antibodies: anti-αvβ3, anti-αvβ5, or anti-β1. Following secondary incubation with an anti-mouse FITC-conjugated antibody, cells were detached and analysed with FACS. Data were processed using the WinMDI2.8 software.

binding. However, 38% of inhibition was observed when the G*RGE*SP control peptide was used to compete phage binding to αvβ3. Analogous results were obtained by Ivanenkov *et al*., who observed a significant binding inhibition to αIIbβ3 integrin of phages displaying the EFGC*RGD*MFGC or EFGAC*RGD*CLGA peptide in the presence of the G*RGE*SP peptide (Ivanenkov *et al.,* 1999). Ivanenkov *et al.* relate these data to a nonoptimal conformation and/or exposure of the peptide on the phage for binding to this integrin. It is possible that this is the case also for Pb-phage binding to αvβ3 integrin, as compared to ΔPb phage.

TABLE 2

Differences in Phage Enrichment Yields *in Vivo*

	Binding		Internalisation	
	Pb	ΔPb	Pb	ΔPb
HeLa	8 ± 3	15 ± 6	9 ± 3	40 ± 16
CS-1	1	1	1	1
CS-1/β3	4 ± 1	77 ± 19	2 ± 1	12 ± 3

Note. 7.5 $\times$ 10^4 cells/well were plated and incubated with 10^{12} phage particles. Results are expressed as fold of enrichment with respect to control phage. Each experiment was performed in duplicates and repeated twice: results are inter- and intraexperiments average values. Standard deviation is shown.

To our knowledge, direct Ad or Pb binding to β1 soluble integrins has not yet been described. Nevertheless, indirect evidence has suggested a role of β1 receptors during Ad infection (Croyle *et al.,* 1998; Davison *et al.,* 1997). Our data give insight for a molecular explanation to this evidence.

Differences in binding properties of Pb phage and ΔPb phage were issued from our *in vitro* studies. On αvβ3, αvβ5, and α5β1 integrin subtypes a fivefold higher signal was obtained with ΔPb phage, as compared to Pb phage. Conversely, on α3β1 receptors, a stronger signal was observed for Pb phages, as compared to ΔPb phages. The latter data suggest that the full-length Pb

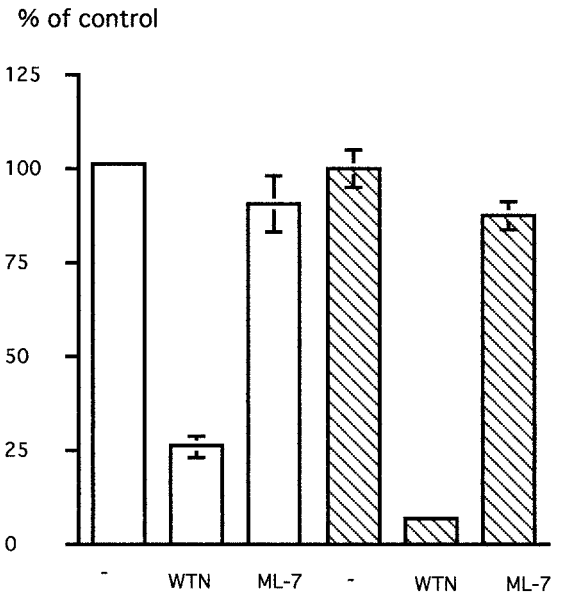

FIG. 6. Effect of kinase inhibitors on phage internalisation. 10^{12} particles of ΔPb phage (white bars) or of Pb phage (stripped bars) were biopanned on HeLa cells. Endocytosed phages were recovered and titrated. Where indicated, cells were incubated in the presence of the inhibitors Wortmannin (WTN, 1 μM) or ML-7 hydrochloride (ML-7, 2 μM). Data are presented as percentage of control enrichments, where infection was performed in the absence of inhibitors. Results are average values from three different experiments performed with duplicates; standard deviation is shown.

molecule includes a binding motif, outside from the central loop, that could mediate or stabilise the Pb/α3β1 interaction.

In a vector-targeting perspective, it is of particular relevance to determine whether recombinant phages bind cells in a receptor-dependent manner, and if they get efficiently internalised. Electron microscopy images offer an original picture of filamentous phages on the surface of cells: no preferential distribution was observed but, as shown in Fig. 3c, an accumulation of filamentous structures was visible in cell invaginations. We did not see filamentous structures when cells where incubated with control virus, but this observation does not exclude per se the presence of nonspecific cell binding of control phages. Immunofluorescence data showed that recombinant phages could get internalised via an energy-dependent process. Both binding and internalisation cytological data were validated in micropanning. This assay presents several advantages: it not only consents straightforward relative quantification of phages binding and internalisation properties, but also permits bound or internalised phage recovery for further analysis and/or selection (Felici *et al.,* 1995). It is interesting to note that, consistently with *in vitro* data, the best Pb-phage versus ΔPb-phage *ratio* is found on β1 receptors expressing cells.

An important question to be addressed was whether the Pb conferred to the phage the ability to activate the endocytic route of adenovirus. Selective pharmacologic disruption indicated that particle uptake of both Pb and Δpb phage depends on the activation of the PI3K kinase, but is independent from myosin light-chain signaling. Interestingly, this pathway overlaps that of adenovirus

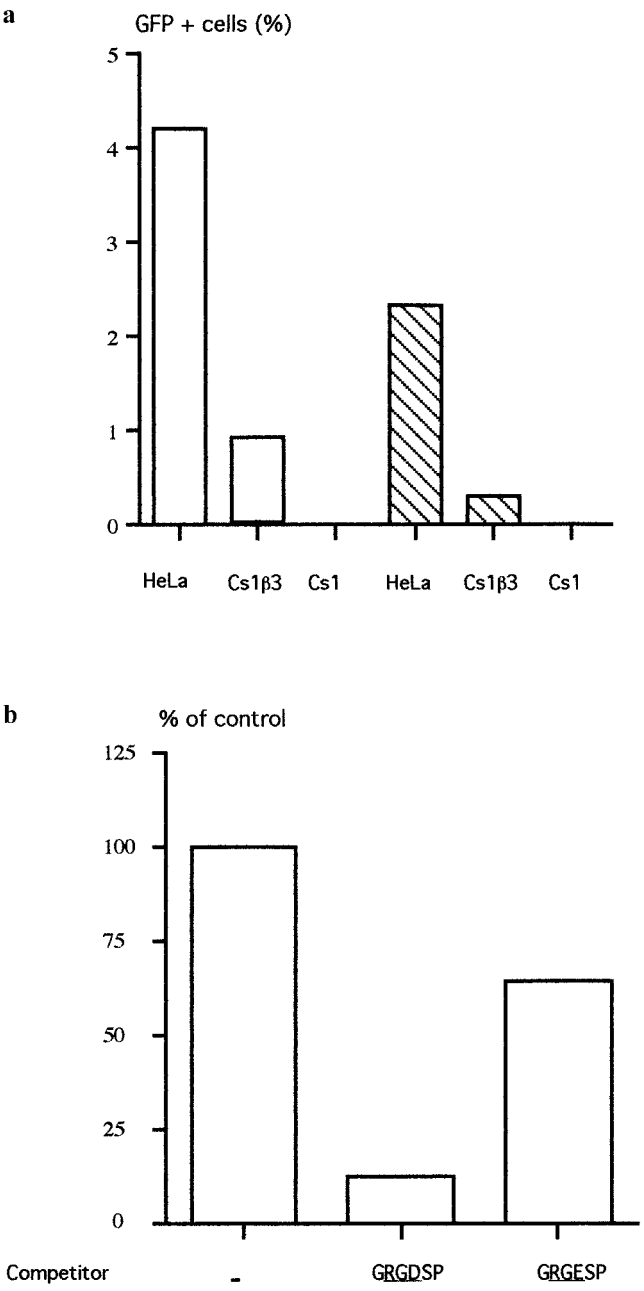

FIG. 7. Recombinant phage can transduce mammalian cells in a receptor-dependent manner. (a) Cells were incubated 1 h at 4°C and 3 h at 37°C with 2×10^{13} particles of Pb-GFP phage or of ΔPb-GFP phage. After 72 h, cells were analysed with FACS. White and stripped bars correspond to ΔPb-GFP-phage and Pb-GFP-phage infection, respectively. (b) Cells were preincubated 1 h at 4°C with G*RGD*SP or G*RGE*SP peptides 4.86 μM, corresponding to a 2000-fold molar excess and then infected 3 h at 37°C with 2×10^{13} particles of ΔPb-GFP phage. After 72 h, cells were analysed with FACS. For each sample 10^4 cells were counted; data were processed using the WinMDI2.8 software.

entry, but not that of integrin activation by natural ligands (Li *et al.,* 1998a).

The last and most crucial point we wanted to assess was whether recombinant phages were able to mediate mammalian cell transduction. We have shown that transduction was receptor dependent, and transgene expression in 4% of HeLa cells infected with the chimeric ΔPb-GFP phage was obtained (Fig. 7a). These results are quite encouraging also when compared to previous reports on phage-mediated delivery to mammalian cells. Larocca *et al.* described that a filamentous phage displaying FGF was able to deliver the GFP in COS-1 cells with a 0.4% transduction efficiency (Larocca *et al.,* 1999). Poul *et al.* showed that approximatively 4% transduction efficiency could be obtained in cells overexpressing the targeted receptor of recombinant phages, i.e., ErbB2 (Poul and Marks, 1999).

A striking gap is observed when Δpb-phage internalisation and transduction efficiencies are compared (100% versus 4%, respectively), suggesting a phage-mediated gene delivery rate-limiting step, different from internalisation. Different processes could impair the efficiency of gene delivery: intracellular viral degradation, inefficient nuclear localisation of the chimeric DNA, or single-stranded DNA inefficiency of transduction. Ad-Pb is awaited to confer endosomal escape and nuclear delivery properties (Hong *et al.,* 1999b). Even though endosomal escape appears to be strictly related to the interaction of Pb molecule with integrin receptors, and the endosomal route of recombinant phages should be that of Ad, further analysis is required to establish whether the Pb molecule is effectively able to confer these properties to the phage. Noticeably, when Pb-phage and ΔPb-phage infected cells were analysed, we could observe perinuclear fluorescence; nevertheless confocal microscopy and *in situ* hybridisation will be needed to determine specific intracellular distribution of phage proteins and DNA. According to Poul and Marks (1999), no significant difference in lipofection was observed when single-stranded and double-stranded DNA were compared. Therefore we do not expect that the use of single-stranded DNA represents a major hurdle in phage-mediated delivery. The identification of the bottleneck in the infection process with chimeric bacteriophage will represent a major advancement step for the development of new generation prokaryotic viral chimeras. The possibility of manipulating different capsidic protein of the same phages could be exploited for inserting peptides with different functions, i.e., not only receptor-binding but also nuclear-delivery and endosomal-escape sequences. This strategy has been proven successful for the improvement of transduction with DNA vectors (Luo and Saltzman, 2000).

In conclusion, we show that it is possible to combine adenoviral penton base cell delivery properties with filamentous phage plasticity for the production of targetable chimeras for mammalian cell transduction. Our data open insights for the use of recombinant phages for gene-therapy application. Two major advantages can be recognised in this type of vectors: (i) receptor selectivity, and (ii) easy and low-cost viral manipulation.

MATERIALS AND METHODS

Cells and viruses

HeLa cells (ATCC No. CCL-2) were cultured in DMEM/10% fetal calf serum (FCS). CS-1 and CS-1/β3 were a kind gift of C. Damsky. Cs-1/β5 were kindly provided by Dr. Cheresh. CS-1 cells were cultured in RPMI 1640/10% FCS, and CS-1/β3 and Cs-1/β5 were cultured in RPMI 1640/10% FCS/G418 (Geneticin, Sigma, St. Louis, MO) 500 μg/ml.

Adenovirus was an Ad5-derived ΔE1ΔE3 recombinant; AdRSVβgal was a kind gift of M. Perricaudet. Viral particles were CsCl-purified after amplification as previously described (Stratford-Perricaudet *et al.,* 1992).

Structure prediction analysis

Multiple alignment of Ad-Pb proteins from different serotypes was performed with the Pile-up program of the Genetic Computer Group package using default parameters values (Devereux *et al.,* 1984). Secondary structure predictions were extracted from the PredictProtein server, http://www.embl-heidelberg.de/predictprotein/predictiprotein.html (Rost, 1996), performed with the PHD program both for Ad Pb protein and for multiple alignment (Rost and Sander, 1993, 1994).

Phages

Pb (1–571) and Pb (286–393) fragments were obtained by PCR on Ad2 DNA (Sigma) using the following oligonucleotides pairs: GATCGTCGACATGCAGCGCGCGGCGATGTATGAGG/TGACGCGGCCGCCCTAAAAAGTGCGGCTCGATAGGACGCGC, to amplify the full-length Pb gene, and GATCGTCGACCTGTTGGATGTGGACGCCTACCAGGCA/TGACGCGGCCGCCCTATAGGTTGTAACTGCGTTTCTTGCTGTC, for amplification of the cDNA corresponding to the Pb (286–393) fragment. PCR products were inserted in the vector pHenΔ in the *Sal*I–*Not*I restriction sites (Saggio *et al.,* 1995a). Control phage was prepared from pHenΔ-transformed bacterial cells. All phages were prepared from transfected *Escherichia coli* XI1-blue cells (Stratagene, La Jolla, CA), superinfected with M13 KO7 helper phage (Amersham-Pharmacia Biotech, Uppsala, Sweden). Following superinfection, bacterial supernatants were PEG-precipitated and phage particles were CsCl-purified (Saggio *et al.,* 1995a).

To obtain green fluorescent protein expressing phages, a CMV-GFP-poly(A) cassette was excised from the plasmid pITRUF5-N (kindly provided by N. La Monica). The cassette was subcloned in the recombi-

nant phagemids Pb(1–571)-pHenΔ and Pb(286–393)-pHenΔ, previously digested with *Eco*RI and treated with Klenow enzyme (Roche Diagnostics, Mannheim, Germany) to obtain blunt ends. Recombinant phages were produced after transformation *E. coli* XI1-blue cells and subsequent superinfection, as detailed above.

Western blotting of recombinant phages

Purified phages or Ad particles were loaded on SDS gel. Proteins were Coomassie blue stained or blotted on a nitrocellulose filter, blocked in TBS/5% milk/0.05% Tween 20 (TBSMT), and then incubated with a polyclonal anti-Pb antibody (a kind gift of P. Boulanger) diluted 1:1000 in TBSMT. Following a secondary incubation with an anti-rabbit HRP-conjugated monoclonal antibody (Amersham-Pharmacia Biotech), peroxidase was detected using ECL+ system kit (Amersham-Pharmacia Biotech).

Protein quantification was performed as follows. Coomassie blue and ECL+ signal intensity of different samples were determined with a Phoretix1 program. To avoid loading artifacts, phage content of different lanes was evaluated taking into account the pVIII protein signals of different phages. Giving the arbitrary value of 1 to the pVIII signal of control phages, values of 1.18 and of 1.15 were calculated for Pb phage and ΔPb phage, respectively. In the blot, corrected recombinant pIII signals were compared to the Ad-Pb band. Calculations were performed considering that 1.2×10^9 Ad particles and 1.2×10^{12} phage particles were loaded, corresponding to 7.2×10^{10} Pb molecules and to 4.8×10^{12} pIII molecules, respectively.

Binding to integrin receptors *in vitro*

Purified soluble $\alpha v\beta 3$, $\alpha v\beta 5$, $\alpha 5\beta 1$, and $\alpha 3\beta 1$ were provided by Chemicon (Temecula, CA). Ninety-six-well plates were coated overnight at 4°C with purified integrins. Following washing and blocking in TBSMT supplemented with Ca^{2+} (TBSMT+), phages were added to the wells. In competition experiments, integrins were preincubated, 1 h prior to phage addition, with G*RGD*SP or G*RGE*SP peptides (Sigma). After 2-h incubation and successive washing, attached phages were detected with an anti-M13 pVIII monoclonal antibody (Amersham-Pharmacia Biotech), diluted 1:500 in TBSMT+. After secondary incubation with anti-mouse HRP-conjugated monoclonal antibody (Amersham-Pharmacia Biotech) diluted 1:1000 in TBSMT+, HRP was detected with TMB liquid substrate (Sigma). Optical reading was performed at 450 nm with an ELISA Microplate Reader (Bio-Rad, Hercules, CA).

Binding and internalisation of phages *in vivo*

Electron microscopy. Forty-eight hours before treatment with phages, 10^5 HeLa cells were plated in chambers slides for cell culture (Lab-Tek Chamber slides, NalGe Nunc International, Naperville IL). Added were 3×10^{12} for control phage or ΔPb phage and 9×10^{12} particles of Pb phage. After phage incubation 1 h at 4°C, cells were washed and fixed 10 min in 2% glutaraldehyde in 0.15 M HEPES, pH 7.3. Cells were postfixed for 1 h at room temperature in 1% osmium tetra oxide and 1.5% potassium ferrocyanide in 0.1 M cacodylate buffer, pH 7.3. Cells were dehydrated in a series of alcohols and embedded in Epon 812 resin. Ultrathin sections were stained with uranyl acetate and lead citrate and observed in a transmission electron microscope (CM100; Philips, Eindhoven, The Netherlands).

Immunofluorescence analysis. Plated were 2.5×10^5 HeLa cells on coverslips in six-well tissue culture plates in DMEM/10% FCS. After 48 h, cells were incubated at 4°C with phage particles in PBS+/5% FCS. When required, incubation was continued 1 h at 37°C in the presence of 100 μM chloroquine (Sigma). Following washing with ice-cold PBS+/5% FCS, cells were fixed in PBS+/3.7% formaldehyde and permeabilized, when required, with PBS+/0.1% Triton X-100. After washing and blocking in PBS/0.01% Tween 20/5% milk, cells were incubated with mouse monoclonal anti-M13 antibody (Amersham-Pharmacia Biotech), diluted 1:50 in blocking buffer. Following washing, cells were incubated with FITC-conjugated anti-mouse antibody (Dako, Denmark), diluted 1:50 in blocking buffer. Cells were examined using a fluorescence microscopy with a 40× objective. Photographs were taken with a CCD camera using fluorescein filter set and processed with the Adobe-Photoshop software.

FACS analysis for integrin receptors expression

Plated were 1.5×10^5 cells/well in six-well tissue culture plates. After 24 h, cells were blocked 2 h in PBS/FCS 5% at 4°C. After washing, cells were incubated at 4°C with one of the following primary antibodies: anti-$\alpha v\beta 3$ (1:1000; Chemicon Inc.), anti-$\alpha v\beta 5$ (1:500; Chemicon Inc.), anti-$\beta 1$ (1:1000; Immunotech Inc.), diluted in PBS/FCS 5%. Subsequently, cells were incubated with an anti-mouse FITC-conjugated antibody (Dako), diluted 1:100 in PBS/FCS 5%. Cells were analysed by FACS. Data were processed using the WinMDI2.8 software.

Phage micropanning *in vivo*

Twenty-four-well tissue culture plates were plated with 7.5×10^4 cells/well. After 2 days, medium was removed and cells were incubated at 4°C with phage particles in PBS+/FCS 5%. To detect bound particles, after washing, phages were eluted with 6 M urea/1 N HCl/pH 2.2 at 4°C for 10 min. After neutralisation, eluates were titrated by ELISA. Briefly, 96-well microplates were coated with anti-M13 polyclonal antibody (kindly provided by P. Monaci), serial dilutions of a reference phage or eluates were

tested in TBSMT. Secondary incubation with an anti-M13 pVIII HRP-conjugated monoclonal antibody (Amersham-Pharmacia Biotech) allowed phage detection. Optical density values were converted into phage particle concentration on the basis of the standard curve. To enrich for internalised phages, cells were preincubated for 30 min at 37°C with chloroquine 100 μM (Sigma) alone or in the presence of Wortmannin 1 μM (Sigma) or ML-7 hydrochloride 2 μM (Calbiochem, La Jolla, CA). Cells were then incubated with phages diluted in PBS+/FCS 5%, with chloroquine 100 μM, with or without the inhibitors, 1 h at 4°C, and then 2 h at 37°C. After two elution steps performed in 6 M urea/1 N HCl/pH 2.2, and successive washing, cells were trypsinized and resuspended in lysis buffer (10 mM Tris–HCl/2 mM EDTA/2% DOCNa/pH 8.0). Cell lysates were titrated for phage content by infection of bacterial cells.

FACS analysis for detection of green fluorescent protein

Plated were 1×10^5 cells/well in six-well tissue culture plates. After 24 h, cells were incubated 1 h at 4°C and 3 h at 37°C with 2×10^{13} particles of Pb-GFP phage or of ΔPb-GFP phage. After washing and 72 h incubation in fresh medium, cells were analysed by FACS. For competition experiments, cells were preincubated 1 h at 4°C with G*RGD*SP or G*RGE*SP peptides (Sigma), 4.86 μM, corresponding to a 2000-fold molar excess. Competitor peptides were also kept during subsequent incubations with phages. For each sample 10^4 cells were counted; data were processed using the WinMDI2.8 software.

ACKNOWLEDGMENTS

We thank Paolo Monaci for the generous gift of materials. We are obliged to Letizia Zaccaria for helpful scientific discussion and to Laurence Cordier and Mariam Andrawiss for critical reading of the manuscript. This work was supported by grants from CNR Progetto Finalizzato Biotecnologie (P.n. 115.35154 and 115.23287), from CIB (Consorzio Interuniversitario Biotecnologie), and from Cenci-Bolognetti. Yuri Martina is a recipient of a Cenci-Bolognetti fellowship.

REFERENCES

Croyle, M., Walter, E., Janich, S., Roessler, B. and Amidon, G. (1998). Role of integrin expression in adenovirus-mediated gene delivery to the intestinal epithelium. *Hum. Gene Ther.* **9**, 561–573.

Davison, E., Diaz, R., Hart, I., Santis, G., and Marshall, J. (1997). Integrin $\alpha 5\beta 1$-mediated Adenovirus infection is enhanced by the integrin-activating antibody TS2/16. *J. Virol.* **71,** 6204–6207.

Devereux, J., Haeberli, P., and Smithies, O. (1984). A comprehensive set of sequence analysis programs for the VAX. *Nucleic Acids Res.* **12,** 387–395.

Dmitriev, I., Krasnykh, V., Miller, C., M, W., Kashentseva, E., Mikheeva, G., Belousova, N., and Curiel, D. (1998). An adenovirus vector with genetically modified fibers demonstrates expanded tropism via utilization of a coxsackievirus and adenovirus receptor-independent cell entry mechanism. *J. Virol.* **72,** 9706–9713.

Elliott, G., and O'Hare, P. (1997). Intercellular trafficking and protein delivery by a Herpesvirus structural protein. *Cell* **88,** 223–233.

Felici, F., Luzzago, A., Monaci, P., Nicosia, A., Sollazzo, M., and Traboni, C. (1995). Petide and protein display on the surface of filamentous bacteriophage. *Biotech. Ann. Rev.* **1,** 149–183.

Harari, O., Wickham, T., Stocker, C., Kovesdi, I., Segal, D., Huehns, T., Sarraf, C., and Haskard, D. (1999). Targeting an aenoviral gene vector to cytokine activated vascular endotelium via E-selectin. *Gene Ther.* **6,** 801–807.

Hogenboom, H. R., Griffiths, A. D., Johnson, K. S., Chiswell, D. J., Hudson, P., and Winter, G. (1991). Multi-subunit proteins on the surface of filamentous phage: methodologies for displaying antibody (Fab) heavy and light chains. *Nucleic Acids Res.* **19,** 4133–4137.

Hong, S., Galaup, A., Peytavi, R., Chazal, N., and Boulanger, P. (1999a). Enhancement of adenovirus-mediated gene delivery by use of an oligopeptide with dual binding specificity. *Hum. Gene Ther.* **10,** 2577–2586.

Hong, S., Gay, B., Karayan, L., Dabauvalle, M., and Boulanger, P. (1999b). Cellular uptake and nuclear delivery of recombinant adenovirus penton base. *Virology* **262,** 163–177.

Huang, S., Kamata, T., Takada, Y., Ruggeri, Z., and Nemrow, G. (1996). Adenovirus interaction with distinct integrins mediates separate events in cell entry and gene delivery to hematopoietic cells. *J. Virol.* **70,** 4502–4508.

Hufton, S., Meulemans, E., de Bruine, A., Arends, J., and Hoogenboom, H. (1999). Phage display of cDNA repertoires: The pVI display system and its applications for the selection of immunogenic ligands. *J. Immunol. Methods* **231,** 39–51.

Ivanenkov, V., Felici, F., and Menon, A. (1999). Uptake and intracellular fate of phage display vectors in mammalian cells. *Biochim. Biophys. Acta* **1148,** 450–462.

Kassner, P., Burg, MA, Baird, A, Larocca, D (1999). Genetic selection of phage engineered for receptor-mediated gene transfer to mammalian cells. *Biochem. Biophys. Res. Commun.* **264,** 921–928.

Larocca, D., Kassner, P., Witte, A., Ladner, R., Pierce, G., and Baird, A. (1999). Gene transfer to mammalian cells using genetically targeted filamentous bacteriophage. *FASEB J.* **6,** 727–734.

Larocca, D., Witte, A., Johnoson, W., Pierce, G. F., and Baird, A. (1998). Targeting bacteriophage to mammalian cell surface receptors for gene delivery. *Hum. Gene Ther.* **9,** 2393–2399.

Li, E., Stupack, D., Klemke, R., Cheresh, D., and Nemerow, G. (1998a). Adenovirus endocytosis via αv integrins requires phosphoinositide-3-OH kinase. *J. Virol.* **72,** 2055–2061.

Li, E., Stupak, D., Bokoch, G., and Nemerow, G. (1998b). Adenovirus endocytosis requires actin cytoskeleton reorganizaion mediated by the Rho family GTPases. *J. Virol.* **72,** 8806–8812.

Lowman, H., Bass, S., Simpson, N., and Wells, J. (1991). Selecting high affinity binding proteins by monovalent phage display. *Biochemistry* **30,** 10832–10838.

Lowman, H. B., and Wells, J. A. (1993). Affinity maturation of human growth hormone by monovalent phage display. *J. Mol. Biol.* **234,** 564–578.

Luo, D., and Saltzman, W. (2000). Synthetic DNA delivery systems. *Nature Biotech.* **18,** 33–37.

Mathias, P., Galleno, M., and Nemerow, G. (1998). Interactions of soluble recombinant integrin $\alpha v\beta 5$ with human Adenovirus. *J. Virol.* **72,** 8669–8675.

Poul, M., and Marks, J. (1999). Targeted gene delivery to mammalian cells by filamentous phage. *J. Mol. Biol.* **288,** 203–211.

Reynolds, P., Dimtriev, I., and Curiel, D. (1999). Insertion of an RGD motif into the HI loop of adenovirus fiber protein alters the distribution of transgene expression of the systhemically administered vector. *Gene Ther.* **6,** 1336–1339.

Roelvink, P., Lee, G., Einfeld, D., Kovesdi, I., and Wickham, T. (1999). Identification of a conserved receptor-binding site on the fiber proteins of CAR-recognizing adenovirus. *Science* **286,** 1568–1571.

Rost, B. (1996). PHD: Predicting one-dimensional protein structure by profile based neural networks. *Methods Enzymol.* **266,** 525–539.

Rost, B., and Sander, C. (1993). Prediction of protein secondary structure at better than 70% accuracy. *J. Mol. Biol.* **232,** 584–599.

Rost, B., and Sander, C. (1994). Combining evolutionary information and neural networks to predict protein secondary structure. *Proteins* **19,** 55–77.

Russel, S., and Cosset, F. (1999). Modifying the host range properties of retroviral vectors. *J. Gen. Med.* **1,** 300–311.

Saggio, I., Gloaguen, I., and Laufer, R. (1995a). Functional phage display of ciliary neurotrophic factor. *Gene* **152,** 35–39.

Saggio, I., Gloaguen, I., Poiana, G., and Laufer, R. (1995b). CNTF variants with increased biological potency and receptor selectivity define a functional site of receptor interaction. *EMBO J.* **14,** 3045–3054.

Saitoh, M., Ishikawa, S., Matsushima, S., Naka, M., and Hidaka, H. (1987). Selective inhibition of catalythic activity of smooth muscle myosin light chain kinase. *J. Biol. Chem.* **262,** 7796–7801.

Stewart, P., Chiu, C., Huang, S., Muir, T., Zhao, Y., Chait, B., Mathias, P., and Nemerow, G. (1997). Cryo-EM visualization of an exposed RGD epitope on adenovirus that escapes antibody neutralization. *EMBO J.* **16,** 1189–1198.

Stratford-Perricaudet, L. D., Makeh, I., Perricaudet, M., and Briand, P. (1992). Widespread long-term gene transfer to mouse skeletal muscles and heart. *J. Clin. Invest.* **90,** 626–630.

Ui, M., Okada, K., Hazeki, K., and Hazeki, O. (1995). Wortmannin as a unique probe for an intracellular signalling protein, phosphoinositide 3-kinase. *Trends Biochem. Sci.* **20,** 303–307.

Wickham, T., Filardo, J., Cheresh, D., and Nemerow, G. (1994). Integrin $\alpha v\beta 5$ selectively promotes adenovirus mediated cell membrane permealization. *J. Cell Biol.* **127,** 257–264.

Wickham, T. J., Mathias, P., Cheresh, D. A., and Nemerow, G. R. (1993). Integrins $\alpha v\beta 3$ and $\alpha v\beta 5$ promote adenovirus internalization but not virus attachment. *Cell* **73,** 309–319.

Zhang, H., Bilbao, G., Zhou, T., Contreras, J. L., Gomez-Navarro, J., Feng, M., Saito, I., Mounts, J. D., and Curiel, D. T. (1998). Application of a Fas-ligand encoding a recombinant adenovirus vector for prolongation of transgene expression. *J. Virol.* **72,** 2483–2490.